Monatshefte für Chemie 133, 1469–1480 (2002)
DOI 10.1007/s00706-002-0512-9

Monatshefte für Chemie
Chemical Monthly
Printed in Austria

Stable Monopyrrole Atropisomers

Stefan E. Boiadjiev and **David A. Lightner***

Department of Chemistry, University of Nevada, Reno, Nevada 89557-0020, USA

Received July 1, 2002; accepted July 8, 2002
Published online October 7, 2002

Summary. Malonic ester derivatives of ethyl and methyl 3,5-dimethyl-4-(1′-iodoneopentyl)-1*H*-pyrrole-2-carboxylate exhibit restricted rotation about the pyrrole C(4)–C(1′) bond due to the bulky 1′-*tert*-butyl and malonic ester groups and the *ortho* effect at C(4) of the sterically crowded 3,5-dimethylpyrrole. The malonates belong to a rare class of atropisomers with restricted rotation about an sp^3–sp^2 C–C bond, and they undergo diastereomeric separation by TLC and crystallization: the diastereomers are stable in solution at room temperature. A crystal of one of the diastereomers, suitable for X-ray crystallography, gave the relative configuration of the chiral axis and stereogenic center at C(1′). Dynamic NMR studies of the purified diastereomers provide kinetic and thermodynamic parameters associated with the atropisomerism: $\Delta G^{\ddagger} = 132$–$134\,\mathrm{kJ/mol}$ ($\sim 32\,\mathrm{kcal/mol}$) at 383 K in $C_2D_2Cl_4$ solvent.

Keywords. Pyrrole; Diastereomers; NMR spectroscopy.

Introduction

Typically, atropisomerism is found in biaryls such as 1,1′-binaphthyls and certain 2,2′,6,6′-tetrasubstituted biphenyls, where bond rotation about the sp^2–sp^2 C–C bond is sufficiently restricted so as to lead to separable conformers [1, 2]. Separability here implies a rotational free energy barrier of $>110\,\mathrm{kJ/mol}$ at 300 K and half-life of 1000 s. In contrast, restricted rotation about an sp^2–sp^3 C–C bond has seldom been observed. Certain fluorene atropisomers have been isolated where sufficiently large substituents have been positioned judiciously to restrict bond rotation [1–4]. An even simpler example where atropisomers have been isolated has only one aromatic ring: α,α-di-*tert*-butyl benzyl alcohol (Figure 1A) [5]. Far fewer examples of atropisomerism have been recognized among bipyrroles [6], and none involving restricted rotation about an sp^2–sp^3 C–C bond has been reported for monopyrroles. In the following, we report what we believe to be the first examples (Figure 1B) of configurationally stable sp^2C–sp^3C atropisomers of a monopyrrole.

* Corresponding author. E-mail: lightner@scs.unr.edu

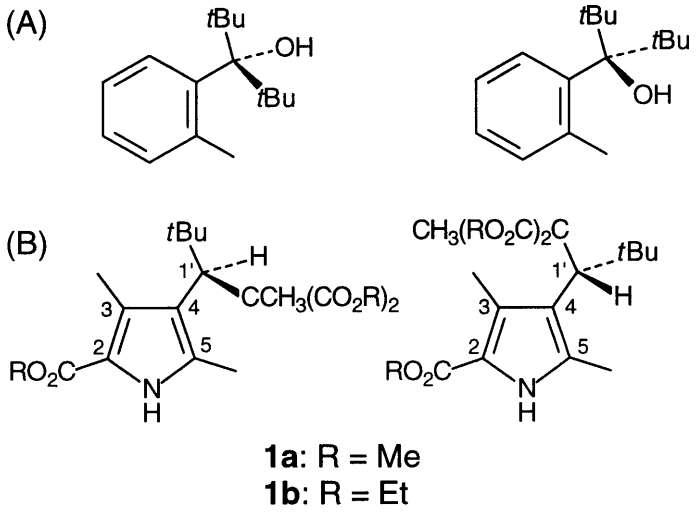

Fig. 1. Isolatable diastereomers, with atropisomerism due to restricted rotation of the sp^2–sp^3 C–C bond in (A) benzene (Ref. [5]) and (B) pyrrole systems. The absolute configuration at 1′ is arbitrary

Results and Discussion

Malonic esters **1a** and **1b** were synthesized in high yield (82–85%) by reaction of dimethyl or diethyl sodio-methylmalonate with methyl or ethyl 1′-iodo-neopentyl-pyrrole-2-carboxylate **2a** or **2b** (Scheme 1). Iodo-pyrrole **2b** was reported over 25 years ago by *Khan* and *Plieninger* [7] from β-free pyrrole **3b** by reaction with pivaldehyde in the presence of HI. We repeated the synthesis of ethyl ester **2b** from **3b** and also prepared methyl ester **2a** from **3a** by the same procedure. The **2a** → **1a** reaction product appeared (by NMR analysis) to be mainly a 79:21 two component mixture, while that from **2b** → **1b** was an 81:19 mixture. Rectification was achieved by radial chromatography followed by crystallization from hexane-ethyl acetate to afford 66 and 56% yields of crystalline **1a** and **1b**, respectively, with NMR spectra consistent with the structures of Fig. 1B. The mother liquors, after careful radial chromatography, afforded material enriched in minor components (**1a**′ and **1b**′). These minor components also gave NMR spectra that correlated

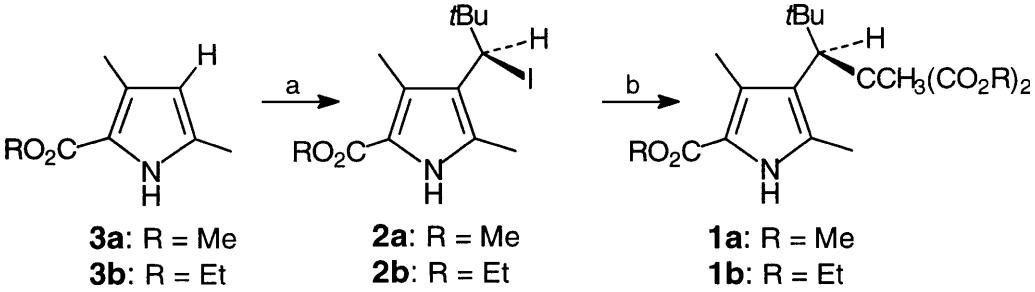

Scheme 1. Reagents: (a) $(CH_3)_3CCHO$, HI, Ac_2O, H_3PO_2; (b) $CHMe(CO_2Me)_2 + NaH/THF$ or $CHMe(CO_2Et)_2 + NaH/THF$

Table 1. Crystal data and structure refinement for pyrrole **1a**

Formula weight	367.43
Crystallized from	*n*-hexane/ethyl acetate
Temperature	298(2) K
Formula	$C_{19}H_{29}NO_6$
Crystal size [mm]	$0.42 \times 0.82 \times 0.60$
Crystal system	Triclinic
Space group	P-1
Z	2
Unit cell dimensions	$a = 8.9721(14)$ Å $\alpha = 97.404(10)^\circ$
	$b = 9.8940(15)$ Å $\beta = 108.564(12)^\circ$
	$c = 11.7482(16)$ Å $\gamma = 92.241\ (10)^\circ$
Volume	976.8(3) Å^3
Density (calculated)	1.249 Mg/m^3
Absorption coefficient	0.092 mm^{-1}
$F(000)$	396
Crystal habit and color	block, colorless
Theta range for data collection	1.85 to 29.90°
Index ranges	$-1 \leq h \leq 10,\ -13 \leq k \leq 11,\ -13 \leq l \leq 13$
Reflections collected	4197
Independent reflections	3466 [R(int) = 0.0158]
Completeness to theta = 29.90°	56.6%
Absorption correction	Empirical
Max. and min. transmission	0.9700 and 0.9561
Refinement method	Full-matrix least-squares on F^2
Data/restraints/parameters	3466/0/236
Goodness-of-fit on F^2	1.084
Final R indices [$I > 2$sigma(I)]	$R1 = 0.0516$, $wR2 = 0.1222$
R indices (all data)	$R1 = 0.0737$, $wR2 = 0.1339$
Largest diff. peak and hole	0.344 and -0.322 e.Å^{-3}
Wavelength	0.71073 Å

nicely with **1a** and **1b**, thus suggesting that the major and minor products have the same constitutional structures and differ only in their stereochemistry.

Crystals of **1a**, grown from slow diffusion of *n*-hexane vapor into ethyl acetate were suitable for X-ray crystallographic structure determination (Table 1). The crystallographic stereostructure and numbering system used are shown in Fig. 2. In **1a**, the hydrogen at C(1), corresponding to C(1′) in Fig. 1B, lies in the plane of the pyrrole ring: H–C(1)–C(4)–C(3) = -1.0° and the *tert*-butyl and methylmalonate groups lie above and below the ring: C(6)–C(1)–C(4)–C(5) = -74.7° and C(10)–C(1)–C(4)–C(5) = 64.6° (Table 2). The C(1)–H is *anti-clinal* to the C(13) methyl group of the methylmalonate unit, with torsion angle H–C(1)–C(10)–C(13) = 158.5°. The C(3)–C(4)–C(1)–C(6) torsion angle is 109.6°; thus the *tert*-butyl group lies almost perpendicular to the plane of the pyrrole ring. From the perspective of Fig. 2, the major diastereomer, **1a**, is the $[(aS,R) + (aR,S)]$ diastereomer.

The dihedral angle C(13)–C(10)–C(1)–C(6) between the methyl group of the methylmalonate and the *tert*-butyl quaternary carbon is 46.5°, an orientation that

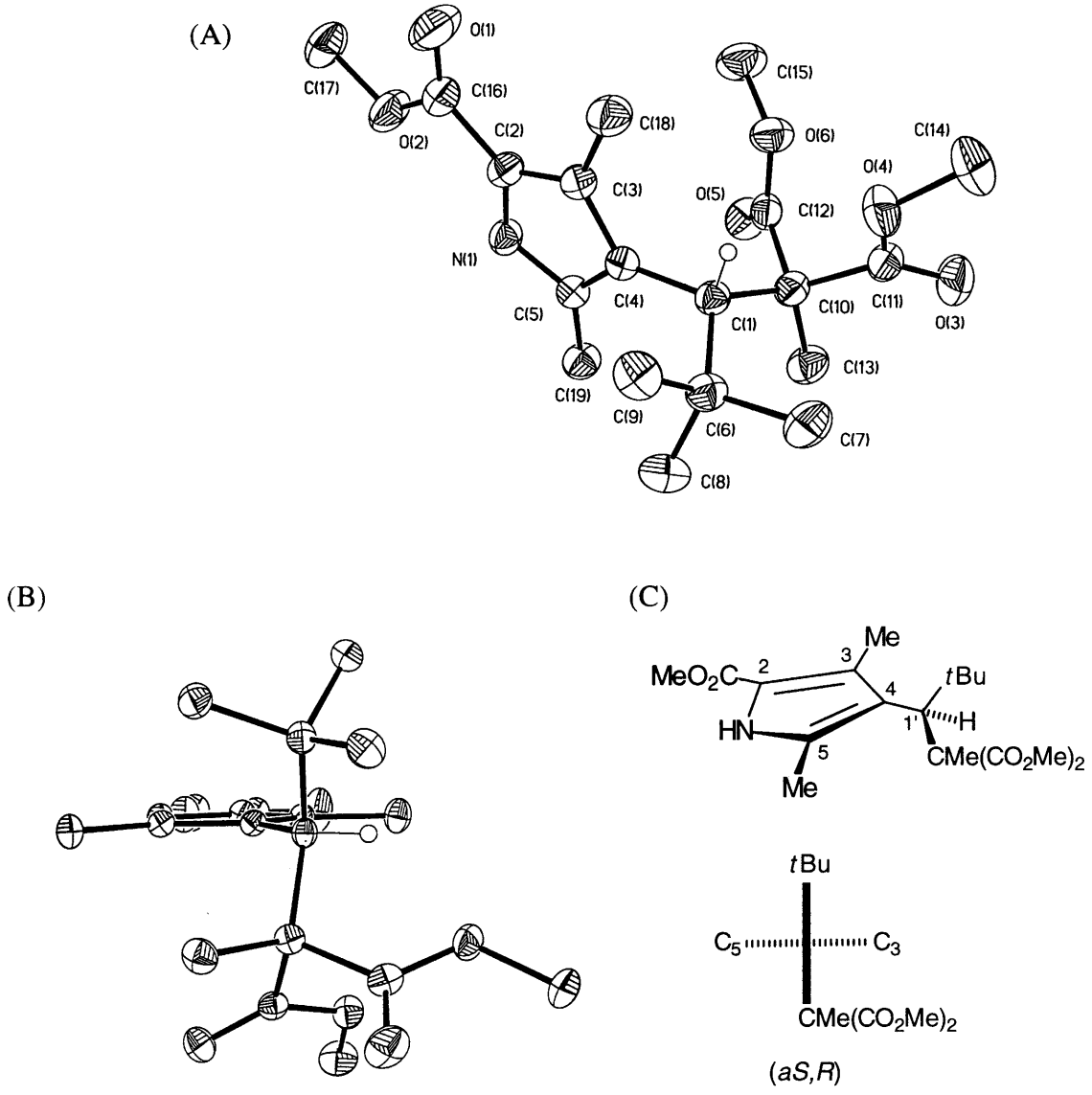

Fig. 2. (A) Structural drawing of major diastereomer of **1a**, and the crystal structure numbering system used. For clarity, only one hydrogen atom is shown: that on the chiral center C(1). (B) Structural drawing of **1a** as viewed from the edge of the pyrrole plane, from C(1) to C(4). (C) Projection diagram that shows the (*aS*) axial chirality configuration. The C(1) stereocenter is (arbitrarily) *R*. Librational ellipsoids have been drawn with 50% probability

places the smallest methine hydrogen flanked by the malonate ester carbonyls and positions the most serically demanding *tert*-butyl group between a methyl and an ester group. The crystal structure shows elongation (1.528 Å) of the C(4)–C(1) bond between the pyrrole ring and sterically crowded stereogenic center bearing the *tert*-butyl relative to other sp^2–sp^3 bond distances from the pyrrole ring to the methyls at C(3) and C(5): C(3)–C(18) = 1.503 Å and C(5)–C(19) = 1.496 Å. There is considerable bond lengthening of the sp^3–sp^3 bonds around C(1): C(1)–C(6) = 1.573 Å and C(1)–C(10) = 1.590 Å *vs.* normal length of 1.53 Å, or more

Table 2. Comparison of conformation determining torsion angles (°) from X-ray crystallography and molecular mechanics[a] calculations of pyrrole **1a**

Torsion angles (°)	X-ray	MMX[a]
H(1B)–C(1)–C(4)–C(3)	− 1.0	− 10.7
C(5)–C(4)–C(1)–C(10)	64.6	60.4
C(6)–C(1)–C(10)–C(13)	46.5	45.7
C(6)–C(1)–C(4)–C(5)	− 74.7	− 87.2
C(6)–C(1)–C(10)–C(12)	166.9	167.5
C(6)–C(1)–C(10)–C(11)	− 79.7	− 75.0
C(4)–C(1)–C(10)–C(11)	142.4	140.3
C(4)–C(1)–C(10)–C(12)	28.9	22.8
C(4)–C(1)–C(10)–C(13)	− 91.5	− 99.0
C(1)–C(4)–C(5)–C(19)	1.7	− 0.4

[a] Using PCModel ver. 7.0, Serena Software, Bloomington, IN USA

specifically: tertiary carbon to quaternary carbon C–C = 1.52 Å and quaternary to quaternary C–C = 1.54 Å. Bond angles around C(1) are also distorted: C(6)–C(1)–C(10) = 117.9° and C(13)–C(10)–C(1) = 117.6°, or considerably opened from the standard tetrahedral valence angle 109.5°. This increases the non-bonded distance between the malonate C(13) methyl and the *tert*-butyl quaternary C(6)–$C(CH_3)_3$ and explains the 46.5° (*vs.* 60°) torsion angle (Fig. 2 and Table 2).

Atropisomerism

Although samples of **1a** and **1b** gave NMR spectra consistent with their structures after purification by crystallization, they showed peak doubling (Fig. 3) of crude mixtures or after pure diastereomers heating above the melting point (160°C), with the spectra consisting of signals from the major and minor isomers (68:32 at equilibrium). Chromatographic analyses of the reaction mixture revealed the presence of the same two components. The behavior and data are consistent with interconversion of the major and minor isomers, which is achieved by rotation about the pyrrole C(4)–C(1′) bond. Such restricted rotation that leads to stable isomers at room temperature, but isomers that interconvert at high temperatures, is consistent with atropisomers having interconversion barriers $>110\,\mathrm{kJ/mol}$ at room temperature. These are apparently the first such examples of sp^2–sp^3 stable atropisomers in monopyrroles.

Interconversion of atropisomeric diastereomers (see Fig. 4) may be expressed as a reversible two-component equilibrium:

$$\mathrm{A} \underset{k_{-1}}{\overset{k_1}{\rightleftharpoons}} \mathrm{A}'$$

which leads to equilibrium expression (1):

$$\frac{[\mathrm{A}]_0 - [\mathrm{A}]_{\mathrm{eq}}}{[\mathrm{A}]_{\mathrm{eq}}} = \frac{k_1}{k_{-1}} = K, \tag{1}$$

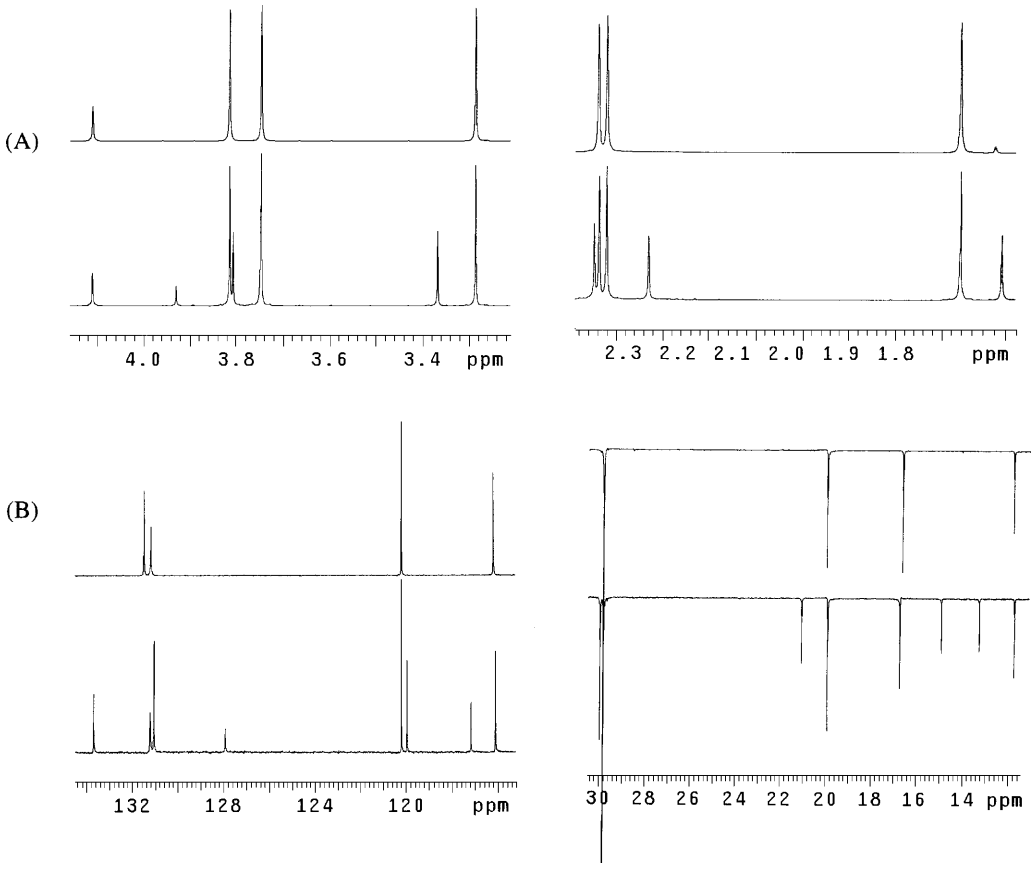

Fig. 3. (A) Partial ^{1}H-NMR spectra of **1a** showing the presence of two diastereomers (lower spectra) in a 67:33 mixture, and pure major diastereomer. (B) Partial ^{13}C-NMR APT spectra of **1a** showing signal doubling in the high field aliphatic region (right) and in the pyrrole ring carbon region (left) for a 67:33 mixture (lower spectrum) and for pure diastereomer (upper spectrum)

where $[A]_0$ and $[A]_{eq}$ are the initial and equilibrium concentrations of one diastereomer, K is the equilibrium constant, and k_1 and k_{-1} are the rate constants for the forward and reverse rates of isomerization.

From the rate law for a reversible isomerization, one may derive an integrated rate expression (2):

$$\ln \frac{[A]_0 - [A]_{eq}}{[A] - [A]_{eq}} = (k_1 + k_{-1})t \tag{2}$$

which is used for extracting kinetic and thermodynamic parameters from NMR intensity data for atropisomerization in solution.

The relative concentrations of the interconverting atropisomers [A] and [A′] are determined by integration of relevant well-separated ^{1}H-NMR signals and followed over time at fixed intervals and at controlled temperatures. At least four pairs of signals were followed, and the mean values of rate constants were used for subsequent energy calculations. The concentrations at equilibrium $[A]_{eq}$ and $[A']_{eq}$ were determined at time ''infinity'' when no further spectral changes were found.

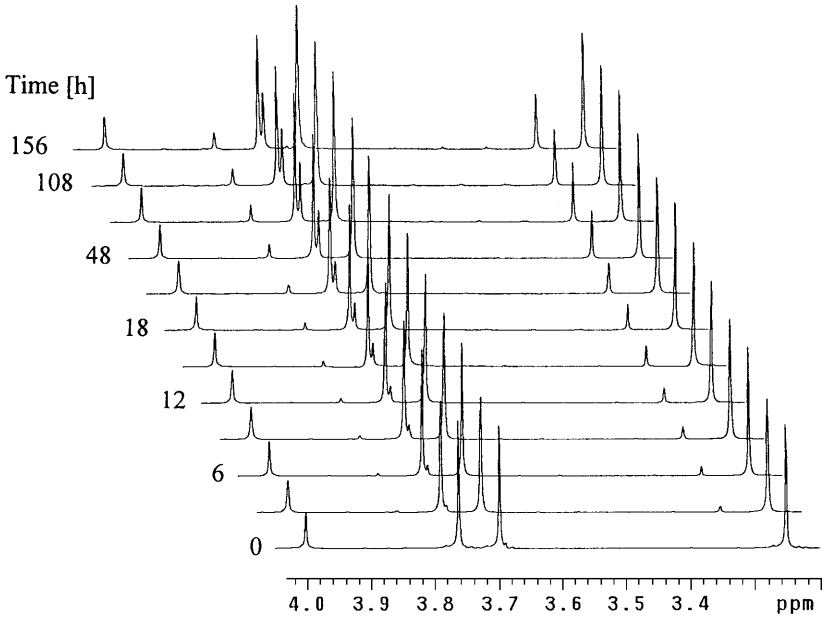

Fig. 4. Partial ^{1}H-NMR spectra of **1a** showing the changes of the C(1′) methine and three OCH_3 proton intensity with time (hours) in $C_2D_2Cl_4$ at 383 K

Plots of $-\ln([A]-[A]_{eq})$ *vs.* time (in seconds) were found to be linear, with slopes equal to (k_1+k_{-1}). Since the ratio $k_1/k_{-1}(=K)$ can be calculated from the equilibrium concentrations (integrals), the individual values of k_1 and k_{-1} could be obtained. The rate constants so determined were used to calculate the free energy of activation ($\Delta G^{\ddagger}$) from the *Eyring* equation: $\Delta G^{\ddagger}=RT[23.76-\ln(k/T)]$ [8]. And the *Gibbs* free energy (ΔG°_{eq}) for the equilibrium is simply the difference between the free energies of activation ($\Delta G^{\ddagger}$) for the forward and backward isomerizations.

Warming diastereomerically pure samples in $CDCl_2CDCl_2$ solvent provided comprehensive sets of NMR data from which kinetic parameters could be computed, as illustrated for **1a**. Quantitative ^{1}H-NMR peak intensities were determined from observations such as those illustrated in Fig. 4 for the C(1′) methine and malonate ester OCH_3 groups. The integrated ratios of pyrrole NH, 1′-H, α-CH_3 and malonate OCH_3 signals were tabulated (Table 3) for atropisomerism in $CDCl_2CDCl_2$ solvent at 383 K, and the computed values of $-\ln([A]-[A]_{eq})$ may be found in Table 4.

Plots of $-\ln([A]-[A]_{eq})$ *vs.* time for the data from Table 4 (see Fig. 5 for example) gave good straight line behavior, and from the slopes of best fit lines for the signals measured (k_1+k_{-1}) was determined. From the measured K_{eq} and (k_1+k_{-1}) values, rate constants k_1 and k_{-1} were determined, and $\Delta G_1^{\ddagger}$ and $\Delta G_{-1}^{\ddagger}$ were calculated (Table 5). The mean values of k_1 ($3.658\cdot10^{-6}\,s^{-1}$) and k_{-1} ($7.928\cdot10^{-6}\,s^{-1}$), and $\Delta G_1^{\ddagger}$ (134.5 kJ/mol) and $\Delta G_{-1}^{\ddagger}$ (132.0 kJ/mol) are consistent with room temperature-stable atropisomers differing in free energy by only ~2 kJ/mol.

Plots of $-\ln([A]-[A]_{eq}$ *vs.* time (s) for **1b** were also linear and along with K_{eq} gave calculated mean $k_1=3.759\cdot10^{-6}\,s^{-1}$ and $k_{-1}=8.389\cdot10^{-6}\,s^{-1}$, or rates

Table 3. ^{1}H-NMR integration ratios for selected diastereotopic hydrogens of **1a** over an equilibration period of 156 hours at 383 K in $CDCl_2CDCl_2$ solvent

Measurement	Time	NMR signal intensity							
	$(s \cdot 10^{-3})$	NH		1′-CH		One of		α-CH_3	
		8.57[a]	8.42[a]	3.99[a]	3.82[a]	α-$COOCH_3$		1.58[a]	1.52[a]
						3.33[a]	3.25[a]		
1	10.8	4.0	96.0	96.6	3.4	4.2	95.8	95.8	4.2
2	21.6	7.0	93.0	93.9	6.1	6.8	93.2	93.2	6.8
3	32.4	9.0	91.0	90.8	9.2	9.1	90.9	91.4	8.6
4	43.2	11.1	88.9	87.6	12.4	12.1	87.9	88.3	11.7
5	54.0	13.9	86.1	85.3	14.7	14.4	85.6	86.9	13.1
6	64.8	16.3	83.7	82.6	17.4	16.1	83.9	84.4	15.6
7	75.6	19.1	80.9	81.8	18.2	18.6	81.4	82.8	17.2
8	86.4	20.5	79.5	80.3	19.7	20.3	79.7	79.3	20.7
9	100.8	21.7	78.3	78.4	21.6	21.9	78.1	78.3	21.7
10	115.2	23.2	76.8	76.5	23.5	23.1	76.9	76.8	23.2
11	129.6	24.7	75.3	75.7	24.3	24.6	75.4	75.2	24.8
12	151.2	25.9	74.1	74.1	25.9	26.0	74.0	74.3	25.7
13	172.8	27.4	72.6	73.0	27.0	27.6	72.4	73.3	26.7
14	216.0	29.4	70.6	71.2	28.8	29.1	70.9	71.8	28.2
15	302.4	30.3	69.7	68.8	31.2	30.6	69.4	69.4	30.6
16	388.8	31.5	68.5	68.2	31.8	31.6	68.4	68.2	31.8
17	561.6	31.4	68.6	68.4	31.6	31.7	68.3	68.4	31.6
$[A]_{eq}^{b}$			68.6	68.4			68.3	68.4	
K_{eq}^{c}		0.458		0.462		0.464		0.462	

[a] δ, ppm; [b] $[A]_{eq} = [\text{dominant diastereomer}]_{eq}$; [c] average value $K_{eq} = 0.462$ at 383 K

Table 4. Values of $[A] - [A]_{eq}$ and ln $([A] - [A]_{eq})$ for the dominant diastereomer of **1a** during the course of its equilibration in $CDCl_2CDCl_2$ at 383 K

Measurement	$\Delta = [A] - [A]_{eq}$ and ln$([A] - [A]_{eq})$ from ^{1}H-NMR signals at							
	NH		1′-CH		One of		α-CH_3	
	Δ	ln	Δ	ln	α-$COOCH_3$		Δ	ln
					Δ	ln		
1	27.4	3.3105	28.2	3.3393	27.5	3.3142	27.4	3.3105
2	24.4	3.1946	25.5	3.2387	24.9	3.2149	24.8	3.2108
3	22.4	3.1091	22.4	3.1091	22.6	3.1179	23.0	3.1355
4	20.3	3.0106	19.2	2.9549	19.6	2.9755	19.9	2.9907
5	17.5	2.8622	16.9	2.8273	17.4	2.8565	18.5	2.9178
6	15.1	2.7147	14.2	2.6532	15.6	2.7473	16.0	2.7726
7	12.3	2.5096	13.4	2.5953	13.1	2.5726	14.4	2.6672
8	10.9	2.3888	11.9	2.4765	11.4	2.4336	10.9	2.3888
9	9.7	2.2721	10.0	2.3026	9.8	2.2824	9.9	2.2925
10	8.2	2.1041	8.1	2.0919	8.6	2.1518	8.4	2.1282
11	6.7	1.9021	7.3	1.9879	7.1	1.9601	6.8	1.9169
12	5.5	1.7047	5.7	1.7405	5.7	1.7405	5.9	1.7750
13	4.0	1.3863	4.6	1.5261	4.1	1.4110	4.9	1.5892

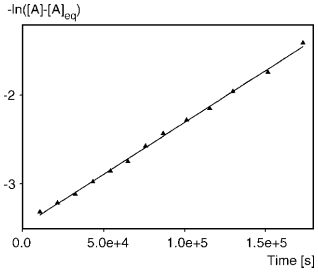

Fig. 5. Plots of $-\ln([A]-[A]_{eq})$ *vs.* time for trimethyl ester **1a** in $CDCl_2CDCl_2$ at 383 K based on changes in the α-$COOCH_3$ methyl signal intensity

Table 5. Summary of thermodynamic and kinetic parameters for the atropisomerism of **1a** at 383 K in $CDCl_2CDCl_2$

	From integration of ^{1}H-NMR signals at				Mean
	NH	1′-CH	One of α-$COOCH_3$	αCH_3	value
Integral ratio at $t \to \infty$	68.6 31.4	68.4 31.6	68.3 31.7	68.4 31.6	
K_{eq}	0.458	0.462	0.464	0.462	0.462
$k_1 + k_{-1}[s^{-1} \cdot 10^5]$	1.198	1.136	1.171	1.131	1.159
intercept	−3.4726	−3.4509	−3.4744	−3.4663	−3.4661
R	0.9983	0.9987	0.9991	0.9953	
k_1 $[s^{-1} \cdot 10^6]$	3.760	3.588	3.710	3.573	3.658
$\Delta G_1^{\ddagger}$ [kJ/mol]	134.4	134.5	134.4	134.6	134.5
k_{-1} $[s^{-1} \cdot 10^6]$	8.215	7.767	7.995	7.733	7.928
$\Delta G_{-1}^{\ddagger}$ [kJ/mol]	131.9	132.1	132.0	132.1	132.0

very similar to those measured for **1a**. From these rate constants the barriers to rotation were determined: for $\mathbf{1b} \rightarrow \mathbf{1b'}$ $\Delta G_1^{\ddagger} = 134.4\,\text{kJ/mol}$ and for $\mathbf{1b} \leftarrow \mathbf{1b'}$ $\Delta G_{-1}^{\ddagger} = 131.8\,\text{kJ/mol}$. The free energies of activation of **1b** are identical to those found for **1a** suggesting a lack of additional steric hindrance from the ethyl *vs.* methyl ester groups.

Experimental

All NMR spectra were obtained on a Varian Unity Plus spectrometer operating at ^{1}H frequency of 500 MHz in $CDCl_3$ solvent (unless otherwise noted). Chemical shifts are reported in δ (ppm) referenced to the residual $CHCl_3$ ^{1}H signal at 7.26 ppm, and $CDCl_3$ ^{13}C signal at 77.00 ppm. The ^{1}H-NMR spectra in $C_2D_2Cl_4$ were referenced to the residual ^{1}H signal at $\delta = 5.94$ ppm. For the dynamic NMR measurements, the probe temperature was controlled by a standard unit of Unity Plus system. A *J*-modulated spin-echo experiment (*A*ttached *P*roton *T*est) was used to assign ^{13}C-NMR spectra. Melting points were taken on a Mel-Temp capillary apparatus and are uncorrected. Gas chromatography-mass spectrometry analyses were carried out on a Hewlett-Packard 5890A capillary gas chromatograph (30 m DB-1 column) equipped with Hewlett-Packard 5970 mass selective detector. Combustion analyses were carried out by Desert Analytics, Tucson, AZ; these results were in favourable agreement with the calculated values. Commercial reagents and HPLC grade solvents were dried and purified following standard procedures [9]. Ethyl 3,5-dimethyl-1*H*-pyrrole-2-carboxylate (**3b**) was synthesized

according to a literature procedure [10], as were the corresponding methyl ester (**3a**) [11] and iodopyrroles **2a** [11] and **2b** [7].

Methyl 3,5-dimethyl-4-[(1′-tert-butyl-2′-carbomethoxy-2′-methyl)methoxycarbonyl-ethyl]-1H-pyrrole-2-carboxylate (**1a**, $C_{19}H_{29}NO_6$)

To a N_2-protected suspension of sodium hydride (900 mg, 30 mmol, 80% oil) in 40 cm^3 of anhydrous *THF* at 10°C was added a solution of 32 mmol of dimethyl methylmalonate in 3 cm^3 of *THF* during 10 min. After stirring for 10 min, 6 mmol of iodide **2a** [11] and 5 cm^3 of *THF* were added and the mixture was heated at reflux for 30 min. After cooling, the mixture was poured into cold 100 cm^3 of 1% aq. HCl and 200 cm^3 of diethyl ether. The aqueous layer was extracted with 2×50 cm^3 of ether and the combined ethereal extracts were washed with water until neutral (3×100 cm^3). After drying over anhydrous $MgSO_4$, filtration and evaporation, the crude mixture of diastereomers was purified by radial chromatography on silica gel eluting with hexane:ethyl acetate = 8:2 to 7:3, (v/v) to yield 85% of pure diastereomers **1a** and **1a′**. Recrystallization from ethyl acetate-hexane afforded pure **1a**. Yield 1.45 g (66%); mp 158–159°C; ^{1}H-NMR: $\delta = 0.98$, (9H, s), 1.67 (3H, s), 2.32 (3H, s), 2.337 (3H, s), 3.27 (3H, s), 3.74 (3H, s), 3.80 (3H, s), 4.10 (1H, s), 8.74 (1H, br.s) ppm; ^{13}C-NMR: $\delta = 11.19$, 16.37, 19.64, 29.80, 37.71, 47.41, 50.85, 52.03, 52.66, 58.68, 116,10, 120.22, 131.04, 133.67, 161.89, 172.06, 173.13 ppm; MS: m/z (%) = 367 [$M^{+\bullet}$] (7), 336 (5), 310 (74), 222 (23), 196 (100), 164 (27); anal. calcd. for $C_{19}H_{29}NO_6$: C 62.10, H 7.96, N 3.81; found: C 62.10, H 8.24, N 3.85.

After being heated at 160°C to melting under N_2 for 24 h, a sample of **1a** in $CDCl_3$ solvent showed (in addition to the signals above) a new set of signals assigned to the minor atropisomer **1a′**. ^{1}H-NMR: $\delta = 1.00$ (9H, s), 1.59 (3H, s), 2.25 (3H, s), 2.339 (3H, s), 3.35 (3H, s), 3.73 (3H, s), 3.79 (3H, s), 3.92 (1H, s), 8.92 (1H, br.s) ppm; ^{13}C-NMR: $\delta = 12.78$, 14.50, 20.82, 29.95, 37.74, 50.05, 50.82, 52.19, 52.56, 58.40, 117.18, 119.98, 127.92, 131.22, 162.00, 172.68, 173.14 ppm.

Ethyl 3,5-dimethyl-4-[(1′-tert-butyl-2′-carboethoxy-2′-methyl)ethoxycarbonylethyl]-1H-pyrrole-2-carboxylate (**1b**, $C_{22}H_{35}NO_6$)

From a pure mixture of diastereomers obtained from **2b** [7] in 82% yield by following the procedure above for **1a**, **1b** was isolated by radial chromatography on silica gel (hexane : ethyl acetate = 8:2 to 7:3) and recrystallizations from ethyl acetate–hexane and methanol–water. Yield 1.38 g (56%); mp 107–108°C; ^{1}H-NMR: $\delta = 0.99$ (9H, s), 1.00 (3H, t, $J = 7.2$ Hz), 1.27 (3H, t, $J = 7.2$ Hz), 1.33 (3H, t, $J = 7.2$ Hz), 1.66 (3H, s), 2.33 (3H, s), 2.34 (3H s), 3.60–3.82 (4H, ABX_3), 4.11 (1H, s), 4.18–4.28 (2H, ABX_3), 8.69 (1H, br.s) ppm; ^{13}C-NMR: $\delta = 11.44$, 13.85, 14.52, 16.36, 19.79, 29.89, 37.80, 46.82, 58.77, 59.61, 61.18, 61.41, 116.24, 120.51, 130.84, 133.46, 161.55, 171.71, 172.71 ppm. MS: m/z (%) = 409 [$M^{+\bullet}$] (2), 364 (2), 352 (61), 279 (3), 236 (30), 234 (37), 224 (100), 188 (31), 57 (21); anal. calcd. for $C_{22}H_{35}NO_6$: C 64.52, H 8.62, N 3.42; found: C 64.63, H 8.76, N 3.66.

After being heated at 150°C to melting under N_2 for 16 h, a sample of **1b** in $CDCl_3$ solvent exhibited (in addition to the signals above) a new set of signals assigned to the minor atropisomer **1b′**. ^{1}H-NMR: $\delta = 1.00$ (9H, s), 1.02 (3H, t, $J = 7.2$ Hz), 1.28 (3H, t, $J = 7.2$ Hz), 1.33 (3H, t, $J = 7.2$ Hz), 1.60 (3H, s), 2.25 (3H, s), 2.36 (3H, s), 3.76–3.82 (4H, ABX_3), 3.94 (1H, s), 4.22–4.32 (2H, ABX_3), 8.87 (1H, br.s) ppm; ^{13}C-NMR: $\delta = 12.96$, 13.52, 14.58, 14.61, 20.79, 30.05, 37.84, 49.46, 58.49, 59.64, 61.15, 61.37, 117.31, 120.26, 127.92, 131.25, 161.74, 172.23, 172.75 ppm.

Kinetics methods

The kinetics of atropisomerism were measured using an oil-bath thermostated aluminum block, which held immersed a thermometer and two sealed NMR tubes containing $1.5 \cdot 10^{-2} M$ solutions in $C_2D_2Cl_4$ at 383 K. The samples were removed from the block every 4 h during the first 48 h

(every 6 h later, or 12 h at the end of the equilibration), quickly cooled, and the ^{1}H-NMR spectra were acquired at 298 K to provide the peak integration data for **1a** $\leftrightarrows$ **1a′** (Table 3) and **1b** $\leftrightarrows$ **1b′**.

X-ray structure and solution

Large (~1.0–1.5 mm) crystals of **1a** were grown by slow diffusion of *n*-hexane vapor into ethyl acetate solution. Suitable crystals were cut to size (0.42 × 0.82 × 0.60 mm) and mounted on a glass fiber, coated with epoxy and placed on the goniometer of a Siemens P4 diffractometer. Unit cell parameters were determined by least squares analysis of 27 reflections with $10.1^\circ < \theta < 25.0^\circ$ using graphite monochromatized MoKα radiation ($\lambda = 0.71073$ Å). A total of 4197 reflections were collected between $3.7^\circ < 2\theta < 59.8^\circ$ yielding 3466 unique reflections ($R_{int} = 0.0158$). The data were corrected for *Lorentz*, polarization effects, and absorption using an empirical model derived from psi scans. Crystal data are given in Table 1. Scattering factors and corrections for anomalous dispersion were taken from a standard source [12]. Calculations were with Siemens SHELXTL Plus (v5.1) software package [13]. The structure was solved by direct methods, in the space group P-1.

All non-hydrogen atoms (Fig. 2, Table 6) were refined with anisotropic thermal parameters. Hydrogen atom positions were calculated using a riding model with a C–H distance fixed at 0.96 Å and a thermal parameter 1.2 times the host atoms. The structure was refined by the full-matrix least

Table 6. Atomic coordinates ($\cdot 10^4$) and equivalent isotropic displacement parameters (Å$^2 \times 10^3$) for **1a**. *U*(eq) is defined as one third of the trace of the orthogonalized U_{ij} tensor

	x	y	z	*U*(eq)
N(1)	5107(2)	4313(2)	3137(2)	40(1)
C(1)	1732(3)	1750(2)	2679(2)	35(1)
C(2)	4081(3)	4558(2)	2045(2)	41(1)
C(3)	2763(3)	3653(2)	1751(2)	38(1)
C(4)	3010(3)	2828(2)	2697(2)	35(1)
C(5)	4480(3)	3282(2)	3549(2)	37(1)
C(6)	2121(3)	228(2)	2419(2)	43(1)
C(7)	733(3)	− 784(3)	2344(3)	57(1)
C(8)	3631(3)	− 177(3)	3312(3)	56(1)
C(9)	2332(3)	38(3)	1164(2)	53(1)
C(10)	967(3)	2125(2)	3716(2)	39(1)
C(11)	− 825(3)	1702(2)	3281(2)	45(1)
C(12)	1085(3)	3702(2)	3978(2)	40(1)
C(13)	1712(3)	1605(3)	4931(2)	52(1)
C(14)	− 3232(3)	1528(3)	1650(3)	69(1)
C(15)	257(4)	5693(3)	3115(3)	69(1)
C(16)	4430(3)	5663(3)	1439(3)	50(1)
C(17)	6288(4)	7468(3)	1547(3)	75(1)
C(18)	1333(3)	3573(3)	638(2)	53(1)
C(19)	5426(3)	2911(3)	4748(2)	46(1)
O(1)	3591(3)	5957(2)	492(2)	81(1)
O(2)	5834(2)	6355(2)	2074(2)	60(1)
O(3)	− 1520(2)	1467(2)	3960(2)	70(1)
O(4)	− 1529(2)	1688(2)	2094(2)	56(1)
O(5)	1917(2)	4382(2)	4904(2)	56(1)
O(6)	144(2)	4219(2)	3047(2)	51(1)

squares method on F^2. A short list of torsion angles may be found in Table 2. Tables of anisotropic displacement parameters, isotropic displacement parameters, atomic coordinates, bond angles and lengths have been deposited at the Cambridge Structure Data File (CCDC No. 186230).

Acknowledgments

We thank the National Institutes of Health (HD-17779) for support of this research. *S. E. Boiadjiev* is on leave from the Institute of Organic Chemistry, Sofia, Bulgaria. Special thanks are accorded to Profs. *J. Nelson* and *V. Catalano* for helpful discussions on the X-ray crystallographic determinations.

References

[1] Eliel EL, Wilen SH, Mander LN (1994) Stereochemistry of organic compounds. Wiley, New York
[2] Ōki M (1983) In: Allinger NL, Eliel EL, Wilen, SH (eds) Topics in stereochemistry, vol 14, Wiley, New York, pp 1–81
[3] Ōki M (1993) The chemistry of rotational isomers. Springer, New York
[4] Kessler H (1970) Angew Chem Int Ed Engl **9**: 219
[5] Lomas JS, Dubois JE (1976) J Org Chem **41**: 3033
[6] Falk H (1989) The chemistry of linear oligopyrroles and bile pigments. Springer, Wien
[7] Khan SA, Plieninger H (1975) Chem Ber **108**: 2475
[8] Günther H (1994) NMR Spectroscopy. Wiley, New York, pp 335–389
[9] Perrin DD, Armarego WLF (1988) Purification of laboratory chemicals, 3rd edn Pergamon Press, England
[10] Robinson JA, McDonald E, Battersby AR (1985) J Chem Soc Perkin Trans **1**, 1699
[11] Boiadjiev SE, Lightner DA (2002) Tetrahedron Asymm, in press
[12] Ibers JA, Hamilton WC (1974) International Tables for X-ray Crystallography, vol 4 Kynoch Press, England
[13] SHELXTL-Plus v5.1, Bruker Analytical X-Ray Systems, Madison, WI, USA

Verleger: Springer-Verlag KG, Sachsenplatz 4–6, A-1201 Wien. – Herausgeber: Österreichische Akademie der Wissenschaften, Dr.-Ignaz-Seipel-Platz 2, A-1010 Wien, und Gesellschaft Österreichischer Chemiker, Eschenbachgasse 9, A-1010 Wien. – Redaktion: Währinger Straße 38, A-1090 Wien. – Satz und Umbruch: Thomson Press Ltd., Chennai, India. – Offsetdruck: Manz Crossmedia, A-1051 Wien. – Verlagsort: Wien. – Herstellungsort: Wien. – Printed in Austria.